

Circumstellar interaction in type Ibn supernovae and SN 2006jc

N.N. Chugai *

Institute of Astronomy, RAS, Pyatnitskaya 48, 119017 Moscow, Russia

Accepted 2009 Received 2009; in original form 2009

ABSTRACT

I analyse peculiar properties of light curve and continua of enigmatic Ibn supernovae, including SN 2006jc, and argue in favour of the early strong circumstellar interaction. This interaction explains the high luminosity and fast flux rise of SN 1999cq, while the cool dense shell formed in shocked ejecta can explain the smooth early continuum of SN 2000er and unusual blue continuum of SN 2006jc. The dust is shown to condense in the cool dense shell at about day 50. Monte Carlo modelling of the He I 7065 Å line profile affected by the dust occultation supports a picture, in which the dust resides in the fragmented cool dense shell, whereas He I lines originate from circumstellar clouds shocked and fragmented in the forward shock wave.

Key words: supernovae: general – supernovae: individual (SN 2006jc) – circumstellar matter

1 INTRODUCTION

Recently a new family of supernovae (SN), so called SN Ibn, came in the limelight (Matheson et al. 2000; Pastorello et al. 2008). These objects, showing strong narrow (FWHM ~ 2000 km s $^{-1}$) He I emission lines and weak or no H α emission, are suggested to be SN Ibc interacting with a helium-rich circumstellar matter (CSM) (Foley et al. 2007; Pastorello et al. 2007; Pastorello et al. 2008). Four known members of this family are: SN 1999cq (Matheson et al. 2000), SN 2000er and SN 2002ao (Pastorello et al. 2008), and well studied SN 2006jc (Nakano et al. 2006; Foley et al. 2007; Pastorello et al. 2007; Di Carlo et al. 2008; Smith et al. 2008; Anupama et al. 2008). In SN 2006jc the CS interaction is manifested also by X-ray emission (Immler et al. 2008). At the position of SN 2006jc an optical transient was detected in Oct. 2004 with the maximal absolute magnitude of $M_R \sim -14$ (Nakano et al. 2006; Foley et al. 2007; Pastorello et al. 2007). This outburst is blamed for the mass ejection by presupernova (Foley et al. 2007; Pastorello et al. 2007).

A striking feature of SN 2006jc is the early dust formation ($t \sim 50$ d) indicated by the infrared emission of hot ($T \sim 1800$ K) dust after about day 50 (Di Carlo et al. 2008; Smith et al. 2008; Mattila et al. 2008) and blue shift of emission lines (Smith et al. 2008; Mattila et al. 2008). Although dust might form in the unshocked ejecta as shown

by Nozawa et al. (2008), the dust formation in the shocked cool dense shell (CDS) seems to be preferred (Mattila et al. 2008). In fact, dust condensation in the CDS has been invoked already for type IIL supernova 1998S (Pozzo et al. 2004).

A general wisdom is that the light of SN 2006jc is powered by the radioactive decay of ^{56}Ni similar to normal SNe Ibc (Tominaga et al. 2008). The X-ray emission is explained by Tominaga et al. (2008) as a result of interaction of SN Ibc ejecta with smoothly distributed rarefied CSM with the total mass of $\sim 0.003 M_{\odot}$. In this model both reverse and forward shocks are adiabatic, i.e., the dust formation in the shocked gas is precluded. In scenario proposed by Mattila et al. (2008) SN 2006jc ejecta collide with a massive $\sim 0.5 M_{\odot}$ CS shell at the distance of 1.5×10^{16} cm. The massive CDS formed in the forward shock was presumably the site where the dust condensed after day 50 (Mattila et al. 2008). Unfortunately authors did not discuss a possible contribution of CS interaction in the bolometric luminosity.

The present study is motivated by the unsettled issue of the dust-forming site and striking facts presently escaped the detailed analysis, viz., (a) luminous maximum and fast pre-maximum flux rise of SN 1999cq; (b) smooth early continuum of SN 2000er; and (c) odd blue continuum of SN 2006jc. The goal of the paper is to propose a model that could account for the above properties and some other observational data, including the dust formation. The paper is organized as follows. Arguments in favour of a strong CS interaction in SNe Ibn at the early stage are considered in Section 2. The

* nchugai@inasan.ru

interaction models with and without ^{56}Ni are then applied to account for the bolometric light curve, X-ray emission, and moderate expansion velocity of outer layers (Section 3). The parameters of the CDS recovered in these models are used to study the dust formation in terms of the theory of homogeneous nucleation (Section 4). The Monte-Carlo simulations of dust occultation effects in He I lines are made to illustrate that the proposed general picture is sensible (Section 5). The results and some worrisome issues are discussed in Section 6.

Hereafter we adopt for SN 2006jc the explosion date 2006 Sep. 21 or JD=2454000 (Mattila et al. 2008) and the distance of 26 Mpc according to redshift from the Lyon Extragalactic Database and assuming $H_0 = 70 \text{ km s}^{-1} \text{ Mpc}^{-1}$.

2 EARLY CS INTERACTION

Pastorello et al. (2008) emphasise the remarkable homogeneity in the spectral properties among SNe Ibn. This fact provides us a confidence that the conclusions made from the analysis of particular objects can be applied to other members of the family. Here I consider observational data which suggest a dominant contribution of CS interaction in the early luminosity and spectra of SNe Ibn.

2.1 Light curve and CSM

Unusually high luminosity of SN 1999cq (type Ibn) at the light maximum with the absolute magnitude $M_R \sim -19.9$ mag (Matheson et al. 2000; Pastorello et al. 2008) and the fast pre-maximum flux rise by > 3 mag in four days (Matheson et al. 2000) are unprecedented for SNe Ibn including luminous SN 1998bw. Both high luminosity and fast brightening suggest that early SN 1999cq was powered by the ejecta interaction with a dense CSM, a scenario similar to that proposed for the early light curve of type IIL SN 1998S (Chugai 2001). SN 2006jc was detected on day 17 after the adopted explosion date (Nakano et al. 2006; Pastorello et al. 2008) and its absolute magnitude at the discovery was similar to that of SN 1999cq at the same age. It seems plausible, therefore, that the predisccovery light curve of SN 2006jc was similar and the early luminosity of SN 2006jc was also affected by the CS interaction. The early interaction should lead to the deceleration of outer layers of ejecta which is supported by the fact that the early ($t < 10$ d) He I 5876 Å emission of SN 2000er shows the maximal expansion velocity of only $\sim 9000 \text{ km s}^{-1}$ (Pastorello et al. 2008), rather moderate value for early SN Ibn.

The total energy radiated by SN 1999cq during the first 10 days after the light maximum is about $E_r \sim 2 \times 10^{49}$ erg according to the available light curve (Matheson et al. 2000; Pastorello et al. 2008). To produce that energy a shock wave with velocity of 10^4 km s^{-1} had to interact with the CS mass of about $M_{cs} \sim 0.02 M_\odot$ assuming 100% radiation efficiency. For that CSM mass enclosed within $r \sim vt \sim 10^{15}$ cm the density parameter for the steady outflow turns out to be $w = M_{cs}/r \sim 4 \times 10^{16} \text{ g cm}^{-1}$. For the density distribution in outer SN ejecta $\rho \propto v^{-9}$ the shocked ejecta should be by 2.5 times more massive (Chevalier 1982b), so the expected CDS mass on day 10 could attain $\sim 0.05 M_\odot$.

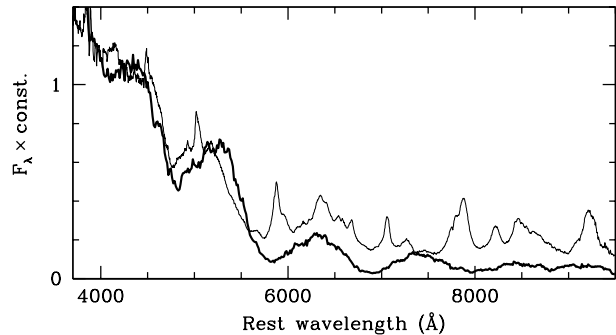


Figure 1. Blue continuum of SN 2006jc on day 22. The model of line emission from cool dense shell (thick solid line) with the reddening $A(V) = 0.15$ is overlaid on the observed spectrum (Fooley et al. 2008).

2.2 Early smooth continuum of SN 2000er

The earliest spectrum of SN 2000er shows a smooth continuum (Pastorello et al. 2008), very unlike bumpy continua of any early SN Ibn. I suggest that the smooth continuum forms in a thin CDS likewise in early SN 1998S (Chugai 2001). The smooth continuum of SN 2000er grows bumpy on the time scale of five days after the first spectrum (Pastorello et al. 2008), which means that the continuum forms in a partially transparent regime, i.e., the optical depth is $\tau \leq 1$. For the luminosity of $\sim 10^{43} \text{ erg s}^{-1}$ on day 10 (Pastorello et al. 2008) and photospheric radius $r \sim vt \sim 10^{15}$ cm the effective temperature of the continuum turns out to be $\sim 10^4$ K.

A question arises, whether a helium-rich CDS with a mass of $\sim 0.05 M_\odot$ is able to maintain a smooth continuum at the age of ~ 10 days? To illustrate the possibility I consider the radiation transfer in the isothermal helium slab with Thomson scattering and absorption taken into account. To facilitate estimates I adopt the LTE approximation. With the boundary condition $F(0) = cU(0)/\sqrt{3}$ (U is the radiation density) is then

$$F_\nu = \frac{4\pi}{\sqrt{3}} B_\nu(T) \frac{\sqrt{\epsilon}(1-E)}{1+E+\sqrt{\epsilon}(1-E)}, \quad (1)$$

where $E = \exp(-\tau\sqrt{3}\epsilon)$, τ is the extinction optical depth and ϵ is the thermalization parameter, i.e., absorption to extinction ratio; both τ and ϵ are functions of frequency. This expression permits us to calculate luminosity of the CDS for a certain gas temperature using Kramers-Unzold approximation for the absorption coefficient of the helium-rich matter.

The density in the CDS is found from the pressure equilibrium adopting the wind density parameter $w = 4 \times 10^{16} \text{ g cm}^{-1}$, shell velocity of 10^4 km s^{-1} , and the radius of $\sim 10^{15}$ cm. To produce the continuum luminosity of $\sim 10^{43} \text{ erg s}^{-1}$ the equation (1) requires the gas of ~ 12500 K for the CDS mass of $0.05 M_\odot$. In the range $\lambda > 4000$ Å the model spectrum is close to black-body with the temperature $T \sim 10200$ K. Although the extinction optical depth of the shell at 6000 Å is only ~ 0.4 the equilibration is rather efficient because thermalization parameter is large $\epsilon > 0.92$ in the range $\lambda > 3000$ Å. We thus conclude that the smooth continuum may arise in early SN Ibn. The epoch of the early

smooth continuum of SN 2006jc preceded the discovery and therefore was missing.

2.3 Blue bumpy continuum at $t \geq 20$ d

The smooth continuum of SN 2000er grew bumpy on a time scale of about one week (Pastorello et al. 2008), although the short period of SN 2000er observations does not permit one to follow the early evolution from smooth till fully developed bumpy continuum we see in SN 2006jc on day 22. No doubt, the bumpy continuum is composed by numerous lines, presumably of Fe II as suggested by Foley et al. (2007). However, unlike any normal SN Ibc, including SN 1998bw, the spectrum of SN 2006jc is unusually blue: the colour $B - R = -0.45$ (Foley et al. 2007) compared with 0.48 of SN 1998bw at the light maximum (Galama et al. 1998). The spectrum also does not show broad absorption lines characteristic of SN Ibc. This indicates that the configuration of "photosphere" surrounded by an extended free expansion atmosphere is irrelevant in this case. Following the picture invoked for the early smooth continuum I assume that the bumpy blue continuum of SN 2006jc arises from the same CDS but this time with the dominant emission in metal lines. This picture is similar to SN 2002ic (Chugai et al. 2004a), so to demonstrate the possibility I use the same model and the same line list of ~ 18000 lines of iron-peak elements in the range of 3500-10000 Å.

The calculated continuum and observed SN 2006jc spectrum on day 22 (Foley et al. 2007) are shown in Fig. 1. The model suggests the emission of randomly oriented plane sheets distributed in the shell $\Delta R/R = 0.1$. The total mass of cold fragments is $0.05 M_{\odot}$ and the solar mass fractions of iron peak elements (Ti, V, Cr, Fe, Ni) are assumed. The adopted expansion velocity is 9000 km s^{-1} , ionization temperature 7000 K, excitation temperature 8000 K, and the area ratio $A = S/4\pi R^2 = 20$. Just to recall, the area ratio is the ratio of cumulative surface area of fragments to the surface area of the CDS; this parameter characterizes a mixing degree. The model spectrum is sensitive to the variation of the excitation temperature within 10% and in lesser extent to the shell mass and thickness, which may vary within 30% without pronounced change of the spectrum. The adopted value of the shell thickness $0.1R$ corresponds approximately to the width of mixing layer formed as a result of a Rayleigh-Taylor instability of the thin shell (Chevalier & Blondin 1995). The model qualitatively reproduces the observed spectrum and bolometric luminosity $\sim 3 \times 10^{42} \text{ erg s}^{-1}$ (cf. Mattila et al. 2008). The high relative intensity of the blue continuum is the result of a larger number of lines per unit wavelength interval in the blue compared to the red part of the spectrum and a weak saturation of intensity in the blue for a moderate area ratio. Given satisfactory fit and sensible values of model parameters, the proposed picture for the blue continuum provides us indirect support for the conjecture of the strong early CS interaction in SNe Ibn.

2.4 CS interaction and emission lines

Spectra of SN 2006jc (Foley et al. 2007; Pastorello et al. 2007) suggest that the velocity of He I line-emitting gas lies in the range of $800 - 6000 \text{ km s}^{-1}$ with the velocity of the

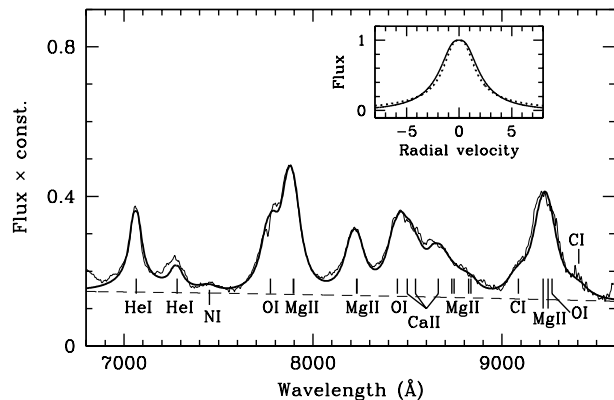


Figure 2. Emission lines in the red part of the spectrum of SN 2006jc on day 22. Thick line shows synthetic spectrum; thin line is the observed spectrum (Fooley et al. 2008); dashed line is adopted continuum. Inset shows profiles used in the synthetic spectrum for He I lines (dotted line) and metal lines (solid line).

bulk of emitting material in the range of $800 - 3000 \text{ km s}^{-1}$. The minimal velocity of $\sim 800 \text{ km s}^{-1}$ could be associated with the cloud shocks speed and perhaps with the velocity of the undisturbed CSM. The latter is about 620 km s^{-1} as indicated by the absorption minimum of narrow lines of O I 7773 Å and He I 6678 Å (Anupama et al. 2008). Interestingly, the expansion velocity of CSM of SN 2000er indicated by narrow He I absorption components in early spectra is $800 - 900 \text{ km s}^{-1}$ (Pastorello et al. 2008), close to this value.

To account for the velocity spectrum of the He I line-emitting gas I suggest that the bulk of the He I emission originates from shocked CS clouds. Two-dimensional hydrodynamic simulations of interstellar cloud engulfed by the blast wave (Klein et al. 1994) prompt us a picture in which the velocities of the line-emitting gas are produced by slow (because of density contrast) radiative shocks of CS clouds in combination with the fragmentation cascade of shocked clouds and acceleration of fragments. This scenario is similar to that proposed for the $H\alpha$ emission in SN 2002ic (Chugai et al. 2004a). The total optical luminosity of He I lines is about $L \sim 5 \times 10^{40} \text{ erg s}^{-1}$ on day 22 (Smith et al. 2008). The corresponding radiation efficiency of the forward shock kinetic luminosity is $\eta = L/(0.5wv_s^3)$. With the forward shock velocity $v_s = 9000 \text{ km s}^{-1}$, wind density parameter $w = 4 \times 10^{16} \text{ g cm}^{-1}$ the required efficiency should be $\eta \sim 0.003$, a reasonable value.

The other emission lines seem to originate from the same line-emitting gas. This is demonstrated by the synthetic spectrum of SN 2006jc on day 22 in which profiles and intensities were adjusted to fit the observed spectrum (Fig. 2). Apart from He I, O I, and Ca II lines the synthetic spectrum includes Mg II lines (Pastorello et al. 2007; Anupama et al. 2008) and two Cl I lines 9088 Å ($^3P^o - ^3P$) and 9406 Å ($^1P^o - ^1D$), which are also pronounced in novae (Williams et al. 1991). There is a vague hint of a weak NI 7452 Å emission with the intensity ratio NI 7452 Å/O I 7773 Å of ~ 0.1 (Fig. 2). The fact that profiles of all the lines are identical confirms that these emissions originate from the same line-emitting gas, which I associate with the shocked CS clouds.

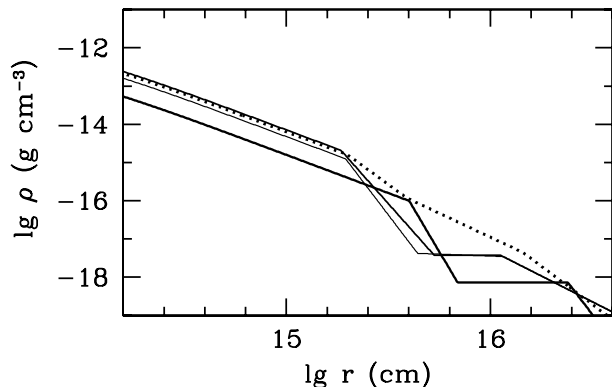


Figure 3. Density distribution of the circumstellar gas for studied models. Thin, intermediate and thick solid lines correspond to the model A1, A3, and A2 respectively, while the dotted line stands for the model B.

3 INTERACTION MODEL

The CS interaction and bolometric light curve are simulated using the model described earlier (Chugai 2001). To recap, the hydrodynamics of the interaction is treated in the thin shell approximation (Chevalier 1982a). The X-ray emissions of the reverse and forward shocks are calculated assuming a homogeneity of each post-shock layer and adopting the cooling function of Sutherland & Dopita (1993). The electron temperature in the postshock gas is calculated taking into account partial Coulomb equilibration. The absorbed and emergent X-ray luminosity is computed assuming the unabsorbed emissivity spectrum to be $\epsilon(E) \propto E^{-0.5} \exp(-E/kT)$ and taking into account the absorption by the cool gas (SN ejecta, CDS and unshocked CSM). The model despite many simplifying assumptions seems to be reasonable which is confirmed by the modelling of SN 1999em X-ray flux (Chugai et al. 2007). The absorbed X-ray luminosity is reprocessed into the ultraviolet (UV), optical, and infrared photons. We adopt that the bulk of this radiation falls in the band in which the observed bolometric light curve is sampled. This assumption is sensible at the early epoch ($t < 1$ month), when the cool gas is opaque in UV region and rather crude at the late epoch ($t \sim 1$ yr), when significant fraction of the reprocessed radiation can escape in UV lines (Chevalier & Fransson 1994). The interaction luminosity combined with the diffusion luminosity of the ejecta produces the model bolometric luminosity. In turn, the diffusion luminosity is modelled using the Arnett (1980) approximation.

A smooth CSM is assumed, neglecting clumpiness, which implies that the calculated luminosity and temperature of the X-ray emission from the forward shock perhaps are not reliable. I present two versions of the interaction model: with ^{56}Ni and without ^{56}Ni . The gamma-ray deposition is calculated assuming that ^{56}Ni is mixed in the inner 90% of the ejecta mass. The ejecta density distribution is approximated by the exponential law $\rho \propto \exp(-v/v_0)$, while the radial density distribution of the CSM is adjusted to describe the bolometric and X-ray luminosities and the radii of the dusty shell associated with the CDS. The composition of major elements is assumed to be He : C : O = 0.9 : 0.06 : 0.04. This choice, called a "standard abundance", is similar to that of Mattila et al. (2008). The pre-SN radius

$R_0 = 10 R_\odot$ is assumed; the exact value is irrelevant, unless the radius is very large, $R_0 \gg 10 R_\odot$.

The Table 1 shows model parameters: the explosion energy, ejecta mass, ^{56}Ni mass, mass of the CS envelope, mass of the CDS formed in the reverse shock by day 50, and the wind density parameter w in the inner region $r < 2 \times 10^{15}$ cm. Our models admit formation of the CDS with a mass of 0.01 – 0.09 M_\odot in the forward shock during initial phase of 5–15 days depending on the model. In a more realistic case of clumpy CSM the situation with the forward shock CDS would become more complicated. Radiative cloud shocks would result in the formation of cool CS gas in a forward shock. However, the expected kinematics and distribution of this cool gas would be essentially different compared to the model of a smooth wind. Models with ^{56}Ni differ by the ejecta parameters and the wind density. It should be stressed that ejecta mass and energy are poorly constrained by the light curve and spectrum. The high energy model A2 corresponds to the preferred model of Tominaga et al. (2008), while the models A1 and A3 have moderate explosion energy. The CSM density distributions for all the models are presented in Fig. 3.

All the models satisfactorily reproduce the observed bolometric light curve (Fig. 4a) including the maximal luminosity of SN 1999cq estimated from M_R magnitude (Pastorello et al. 2008). Note, we do not plot the low-mass model A3 since its behavior repeats that of the model A1 in all the panels of Fig. 4. Models with ^{56}Ni (A1 and A3) reproduce the X-ray flux within 1σ errors (Fig. 4b), while the model A2 with the high energy lies beyond 1σ range. The model B predicts too high X-ray luminosity that exceeds by a factor of $\sim 5 \times 10^2$ the observed X-ray luminosity around day 50. This is a serious problem for the model without ^{56}Ni . Yet one cannot rule out that the clumpiness of CSM, ignored here, might modify the interaction zone in such a way that X-rays were efficiently absorbed. The observed X-ray flux seem to show a drop by a factor 2.5 between the maximum on day ≈ 110 and the epoch of ≈ 135 d (Immler et al. 2008). This drop cannot be reproduced in any of our interaction model, although models A1 and A3 are consistent with observations within 1σ errors. If the drop is real then shocks in CS clouds engulfed by the forward shock layer contribute significantly to the X-ray emission. In this case the drop of X-ray flux could be related with the disappearance of CS clouds beyond the radius $r \sim 10^{16}$ cm.

A massive (0.2 – 0.3 M_\odot) CDS forms by day 50 in all the models (Table 1); the expansion velocity at the age of 50–100 days is $\sim 10^4$ km s $^{-1}$ in models A1, A3 and B and ~ 26000 km s $^{-1}$ in the high-energy model A2 (Fig. 4c). Accordingly, for models A1, A3 and B the CDS radii are close to photometric radii of the dusty shell (Fig. 4d) reported by Mattila et al. (2008), while the high-energy model A2 has essentially larger CDS radius. Interestingly, for the considered models the CDS mass at $t = 5$ d falls in the range 0.05 – 0.06 M_\odot , the value used in Section 2 to analyse the smooth continuum of SN 2000er.

I explored also the model in which the CSM with the mass of 0.1 – 0.5 M_\odot has a structure of a dense thin shell with the radius of 4×10^{15} cm. This choice corresponds to a scenario in which the CS shell was violently ejected with the velocity of 600 km s $^{-1}$ during the outburst two years prior to the SN explosion. In this case the bolometric light curve

Table 1. Parameters of models of SN ejecta and CSM

Model	E 10^{51} erg	M	M_{Ni}	M_{cs} M_{\odot}	$M_{c ds}$	w 10^{16} g/cm
A1	1.5	3	0.12	0.14	0.21	6
A2	10	5	0.2	0.08	0.19	2
A3	1	1	0.3	0.18	0.21	9
B	1.5	3	0	0.27	0.28	8

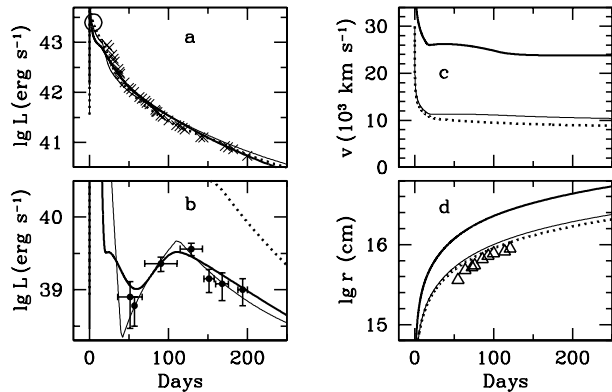


Figure 4. Left panels: Bolometric light curves (a) and X-ray luminosity (b) escaping after absorption in unshocked ejecta, CDS and CSM for the models A1 (thin solid line), A2 (thick solid line) and B (dotted line). Crosses show the observed bolometric light curve according to Pastorello et al. (2008); circle represents the luminosity of SN 1999cq at the light maximum; squares show X-ray luminosity in 0.2-10 keV band (Immler et al. 2008). Right panels: Velocity (c) and radius (d) of the cool dense shell. Triangles show radii of the dusty shell reported by Mattila et al. (2008).

is notably affected by the CS interaction and the model light curve with or without ^{56}Ni is inconsistent with observations.

To summarize, the bolometric light curve of SN 2006jc can be explained by models with and without ^{56}Ni ; both cases suggest the dense wind at the distance $r \leq 2 \times 10^{15}$ cm. In all the models massive CDS forms which might become the dust formation site.

4 DUST FORMATION

For the dust to condense the gas and dust temperatures should become lower than the condensation temperature (T_c). Unfortunately, the CDS gas temperature (T_g) cannot be reliably determined from the radiative energy balance because of complexities of molecular compounds and processes involved. We therefore adopt a sensible assumption that T_g is equal to the radiation temperature $T_r = (F/ac)^{1/4}$, where F is the radiation flux at the CDS radius, a is the radiation constant, c is the speed of light. This approximation probably is not perfect because the gas irradiated by diluted hot radiation is usually warmer than at the radiation temperature. To take into account a possible deviation from the radiation temperature I also consider the case, in which the gas temperature is equal to the dust temperature computed in a formal way; this approximation presumably crudely reflects the physics of heating and cooling of molecular gas. The dust temperature T_d is calculated from the balance be-

tween the absorption of SN radiation and the dust emission. We approximate the SN radiation by the diluted black body spectrum with the temperature of 10^4 K; dust grains are assumed to be graphite spheres with the radius of $0.03 \mu\text{m}$ and the absorption efficiency is set according to Draine & Lee (1984). Calculations show that on day 50 the dust temperature turns out $\sim 10\%$ larger than the radiation temperature.

Given $T_g < T_c$, the dust, nevertheless, forms only, if a characteristic time of the dust formation is essentially smaller than the expansion time. The time scale of the dust formation is determined by the nucleation rate and growth of nuclei due to the gas accretion onto the grains. The rate of the dust growth can be easily estimated using results of the interaction modelling. At the age $t = 50$ d the carbon number density in the CDS for the explored models with standard abundance is $n \sim (2 - 10) \times 10^{11} \text{ cm}^{-3}$ assuming that all the oxygen is bound in CO. Adopting $T_g = 1800$ K and sticking parameter of 0.5 we find that it takes $\sim (1-3) \times 10^2$ s for the dust grains to grow $a \sim 10^{-5}$ cm. This shows that the duration of the dust condensation probably is not constrained by the dust growth.

In line with the theory of homogeneous nucleation (cf. Drain & Salpeter 1977; Hasegawa & Kozasa 1988), the nucleation time scale can be expressed via the number density of dust grains n_g of the final radius a and nucleation rate J

$$t_{nuc} = n_g / J, \quad (2)$$

where $n_g = n\Omega / (4\pi a^3 / 3)$ and $\Omega \sim 2 \times 10^{-23} \text{ cm}^{-3}$ is the volume per carbon atom in a condensed phase. The nucleation rate (Draine & Salpeter 1977; Hasegawa & Kozasa 1988) is defined by the accretion rate onto clusters close to equilibrium point

$$J = \alpha 4\pi r_c^2 u Z n^2 \exp(-16\pi\sigma^3 / 3g^2 kT), \quad (3)$$

where α is the sticking parameter (we adopt $\alpha = 0.5$), Zeldovich factor Z takes into account non-equilibrium distribution of nuclei sizes, u is the average thermal velocity of carbon atoms, $r_c = -2\sigma/g$ is the radius of a cluster of critical size, $\sigma = 1400 \text{ erg cm}^{-2}$ is the energy of graphite surface tension (Tabak et al. 1975), g is the change of free energy in the transition from gas to condensed phase

$$g = -(kT/\Omega) \ln(P/P_{sat}), \quad (4)$$

where P and P_{sat} are the partial pressure and saturation pressure of carbon.

The evolution of partial pressure of carbon and gas temperature for models A2, A3, and B is shown in Fig. 5a. For the model A1, which is not shown, the behavior of calculated values is intermediate between A2 and B. Using a standard expression for Zeldovich factor (cf. Hasegawa & Kozasa 1988) and the partial pressure of carbon from the interaction models one can compute from equations (2-4) the nucleation time (Fig. 5b) for the adopted grain final radius $a = 10^{-5}$ cm. It should be stressed that the result is not sensitive to adopted a . For $a = 10^{-6}$ cm the value $t_{nuc} = 10^4$ s is attained by 0.8 day later. Apart from the standard mixture, we explored also the case of five times higher carbon and oxygen abundance He : C : O = 0.5 : 0.3 : 0.2 (Fig. 5c,d). In this case the nucleation occurs a bit earlier.

A steep time dependence of $t_{nuc}(t)$ function permits us to recover the dust formation epoch for each particular model. Defining the dust formation epoch by the condition

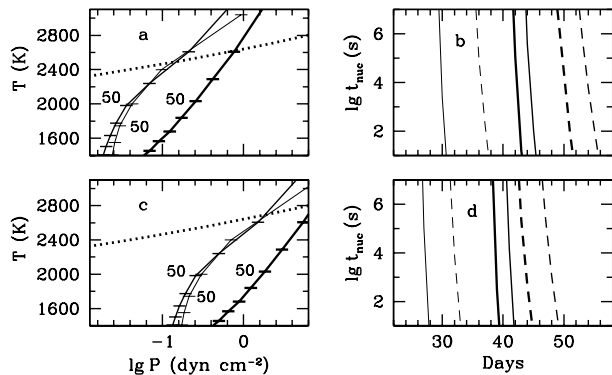


Figure 5. Left panels: Loci of the radiation temperature and pressure in the CDS with the standard composition (upper panel) and five times larger carbon abundance (lower panel). Thick solid line is for model B, intermediate line is for model A2 and thin line is for model A3. Tick marks correspond to every 5 days; the tick on day 50 is indicated. The phase equilibrium for graphite (dotted line) is taken according to Haines & Tsai (2002). Right panel: Evolution of nucleation time in the CDS with the standard composition (upper panel) and five times larger carbon abundance (lower panel). Cases of the gas temperature equal to the radiation and the dust temperature are shown as solid and dashed lines respectively. The line thickness increases along the sequence A3, A2, B.

$t_{nuc} = 1$ day we find for the standard abundance that dust forms between days 42 and 54 for the low energy models and at 30-36 d for the high energy model A2. In the case of five times higher carbon abundance the dust forms at 40-48 d for the low energy models and at 28-32 d for the high energy model. The earlier dust-forming phase in the high energy model is related to the higher CDS velocity, i.e., lower gas temperature at the same age. This modelling shows that the dust forms in the CDS with the standard abundances of He, C, and O at the epoch close to day 50.

The maximal amount of dust for the standard abundance is $\sim 0.005 M_{\odot}$ assuming that all the oxygen is bound in CO molecules and the remaining carbon is converted into the dust. Around day 100 the CDS with the radius of $\sim 10^{16}$ cm (Fig. 4) and the dust mass of $\sim 0.005 M_{\odot}$ has the optical depth $\tau \sim 500$ in R band assuming extinction efficiency $Q_e = 2\pi a/\lambda$. The found upper limit is by a factor of $\sim 10^2$ larger than observational estimates (Mattila et al. 2008) which indicates either low efficiency of the dust formation, or clumpy structure of the dusty shell. Another interesting point is that the one-zone model considered above predicts rapid dust condensation, which is not the case: observations show slow increase of the amount of dust in SN 2006jc (Mattila et al. 2008). This means that conditions in the CDS matter perhaps are not uniform. A spacial variation of the gas temperature is probably a primary factor responsible for the gradual process of the dust condensation.

We considered above the dust formation only in the CDS created by the reverse shock. However, one cannot rule out that the cool gas of shocked CS clouds in the forward shock might be also an appropriate site of the dust formation as well. With some modification this possibility corresponds to the scenario of the dust formation in the cool shell of the forward shock discussed by Mattila et al. (2008).

5 DUSTY SHELL AND BLUE SHIFT

The scenario proposed here suggests that He I emission lines originate from fragmented shocked CS clouds in the forward shock. To simulate line profiles affected by the dust absorption one need to specify the distribution of emissivity and velocity of the line-emitting gas. I suggest that the unabsorbed line profile is determined by the flow of cool fragments of shocked CS clouds in the range $R_1 < r < R_2$, where $R_1 = 1$ is the radius of the CDS, or more precisely, of the contact surface between shocked ejecta and shocked CS gas, and R_2 is the radius of the forward shock front adopted to be 1.25 (cf. Chevalier 1982b). A possible collision of a cloud with the CDS would result in the sudden acceleration of the cloud shock; the shock gets adiabatic and cloud is demolished instantly. The resulting fragments in this case get hot and do not contribute in HeI emission. The integrated emissivity is assumed to be constant in the range $R_1 < r < R_2$, which is sensible approximation, if the bulk of CS clouds crosses the postshock layer before they get completely fragmented.

The velocity distribution of the line-emitting gas generated by CS clouds interaction with the forward shock is not trivial. The shocked cloud acquires a cometary structure with the low velocity core and high velocity tail of fragments (Klein et al. 1994). For particular cloud the flow kinematics is approximately monotonic: the velocity increases from the core towards farmost tail. The smallest fragments have maximal velocities but they also are prone to rapid mixing with the hot gas (Klein et al. 1994). We assume that the smallest fragments of cool gas disappear before they acquire the velocity of the forward postshock flow. From the mass conservation it follows that the average density of cool gas in the tail monotonically decreases with velocity. The combined flow of clouds at different stages of interaction cannot be reduced to a single-valued function $v(r)$. Instead, at the given radius a broad spectrum of velocities $f(v)$ is expected with the minimal velocity corresponding to cloud shock speed $v_1 \sim 10^3$ km s $^{-1}$ and maximal velocity $v_m(r)$ monotonically rising with r and determined by "oldest" shocked clouds that are colliding with the CDS. I adopt the linear law for the maximal velocity $v_m = v_1 + (v_2 - v_1)(r - R_1)$, where v_2 is a fitting parameter. The velocity density distribution function at the given radius is taken in the simple form

$$f(v) = C \left(\frac{v_m - v}{v_2 - v_1} \right), \quad (5)$$

where C is normalizing factor.

The CDS is subject to Rayleigh-Taylor instability, fragmentation, and mixing in the forward shock layer (Chevalier 1982a; Blondin & Ellison 2001), so the dusty CDS material should be spread between the contact surface $R_{d,1} = R_1 = 1$ and some external radius $R_{d,2}$ which is a free parameter. The emission line profiles affected by the dust is simulated here using Monte-Carlo technique. The dust in our model has velocity of the CDS for which we adopt 9000 km s $^{-1}$. This parameter weakly affects the scattered radiation. The Rayleigh phase function and scattering albedo $\omega = 0.6$ are assumed. I checked different values of ω and found only minor differences which refer to the intensity of the broad scattered component. Note, this component, although weak, may be revealed in the polarized light, if the asymmetry of dust distribution is significant. I also tried the phase function dom-

Table 2. Parameters of the line profile model

Day	v_2 km s ⁻¹	τ	$R_{d,1}$	$R_{d,2}$
76	6000	0.07	1	1.1
95	5000	0.4	1	1.1
127	4000	1.1	1	1.2
148	3000	5	1	1.2

inated by back scatter which would be the case, if the dust resides in optically thick clumps. The difference, primarily in scattered component, turns out small.

The optimal model profiles are plotted (Fig. 6) together with observed He I 7065 Å line profile of SN 2006jc for different epochs (Foley et al. 2007). The fit is good for the three first dates and sensible in the last plot. This can be considered as success of the proposed model. The recovered parameter v_2 , extinction optical depth and radii of the dusty shell are given in Table 2. The decrease of v_2 suggests that the contribution of the high velocity line-emitting gas falls with time. Note, the parameter v_2 is determined by unabsorbed blue part of profile and does not depend on the dust distribution and the optical depth. It is not clear whether the decrease of the high-velocity component is related with the cloud fragmentation and fragment acceleration or with the mixing of high velocity fragments in the hot gas. There is a hint that the relative radius of the outer boundary of the dusty shell $R_{d,2}$ increases with time. Interestingly, such a behavior qualitatively agrees with the initial evolution of a mixing layer driven by the Rayleigh-Taylor instability (Chevalier & Blondin 1995; Blondin & Ellison 2001). A detailed comparison with published numerical models is, however, not possible, because the models for SN 2006jc presented here do not have power-law density profiles for the ejecta and the wind.

I explored cases with larger inner radius of the dusty shell, $R_{d,1} > 1$, but found that the fit worsens in this case. This means that in the preferred model the center of the dust layer is shifted inward relative to the center of the line-emitting layer. This is expected in the proposed picture in which most dust originates from the fragmented CDS and the line-emitting gas is related with the shocked CS clouds.

6 DISCUSSION

The proposed scenario of SN Ibn with the strong early CS interaction turns out successful in explaining some unusual observational properties of SNe Ibn. However, until now we ignored some questions that might have interesting consequences for our model. It is worthy, therefore, to pose and briefly discuss challenging issues and, if possible, to impose additional constraints for the model.

6.1 What does power blue continuum?

The proposed interpretation of the blue bumpy continuum suggests that the most emergent optical radiation originates from the CDS. In case, when the interaction luminosity dominates, the energy from the reverse and forward shocks is

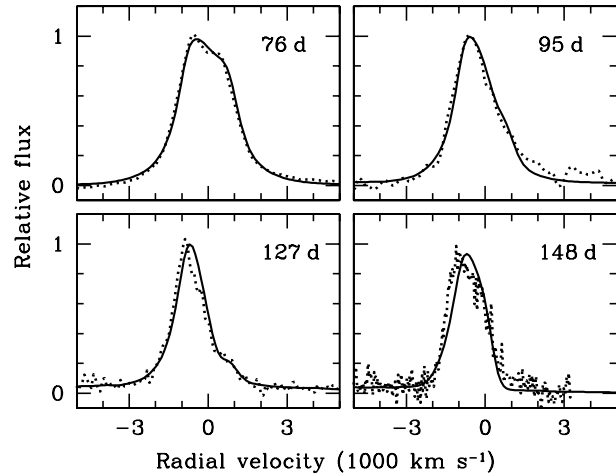


Figure 6. Line profile of He I 7064 Å in SN 2006jc spectra for four epochs. The model and observations (Foley et al. 2008) are shown as a solid line and dotted line, respectively.

deposited into the CDS in a usual way via absorption of X-rays and, perhaps, the thermal conductivity in the mixing zone of the forward shock.

Another possibility could be that the dominant source is ⁵⁶Ni decay. In this case the energy is deposited into CDS owing to the Compton scattering of gamma-quanta and the absorption of ultraviolet radiation emitted by the unshocked ejecta in turn powered by the radioactive decay. The efficiency of the gamma-ray deposition to the CDS is of the order of the ratio of the CDS mass to the mass of ejecta, which is small unless ejecta mass is low $\leq 1 M_{\odot}$.

Alternatively, the CDS gas could be ionized and excited by the absorption of the ultraviolet radiation from the unshocked ejecta. The problem with this mechanism is that in the unshocked freely expanding SN Ibc envelope the ultraviolet radiation is strongly reprocessed by the photon scattering and splitting in numerous ultraviolet metal lines, so the emergent ultraviolet flux gets strongly suppressed relative to visual. The situation in this respect is similar to SNe Ia (cf. Pinto & Eastman 2000). At first glance the ultraviolet flux might become stronger, if the ejecta mass is low. However, for this to be the case the mass should be much lower than that of SNe Ia, i.e., $M < 1 M_{\odot}$. We thus conclude that in the radioactive model the CDS can be the source of the blue continuum, if the ejecta mass is low, $\leq 1 M_{\odot}$.

6.2 Where does He I absorption form?

Helium lines (e.g. 3889 Å) in the blue part of SN 2006jc spectrum show P Cygni profiles with the absorption minimum at ~ -1000 km s⁻¹ and a comparable equivalent width of absorption and emission components (Foley et al. 2007). A natural explanation of this phenomenon is that the continuum in blue region is strong, so the scattering component dominates or comparable with the net line emission. In fact absorption components are also seen in O I 7773 Å and in He I 6678 Å lines (Anupama et al. 2008). The maximal velocity observed in the blue absorption wing of He I 3889 Å line is ≈ 1900 km s⁻¹, three times larger than the wind velocity, $v \approx 600$ km s⁻¹. Apart from the wind, therefore,

an absorbing high velocity component ($> 600 \text{ km s}^{-1}$) is needed to account for the line absorption.

Three possibilities are conceivable for the line-absorbing gas in the range of $600\text{--}2000 \text{ km s}^{-1}$: (a) the CSM in fact has the free expansion kinematics $v \propto r$ with the most material in the range of $600\text{--}2000 \text{ km s}^{-1}$; (b) the line-absorbing gas is simply the same line-emitting gas in the forward shock; (c) the CSM is flow with the constant velocity of $\sim 600 \text{ km s}^{-1}$ but in the preshock zone the CS gas is accelerated up to 1900 km s^{-1} . The first option predicts that the emission lines related with the CSM should get broader with time. In fact, the absorption of He I 3889 Å does not show this trend according to spectra taken by Foley et al. (2007). The second option suggests that fragments of CS clouds in the forward shock should have large covering factor ~ 1 , which is unlikely, although is not ruled out. The third possibility is similar to that suggested for the H α high velocity CS absorption component in early SN 1998S (Chugai et al. 2001), where this feature was attributed to the preshock gas accelerated by either radiation or cosmic rays generated in the forward shock. At the distance of $\sim 10^{16} \text{ cm}$ the radiative force in case of SN 2006jc is weak and cannot accelerate the preshock gas up to more than 100 km s^{-1} in the wind frame and this mechanism should be rejected.

As to cosmic rays, the situation is more optimistic. The point is that in case of clumpy CSM the cosmic ray pressure is build up by the overall shock kinetic luminosity, while the acceleration is applied primarily only to the intercloud gas with a small mass fraction of the inflowing CSM. The intercloud gas, therefore, can acquire significant velocity in the preshock zone. Let ρ_{ic} is the density of the intercloud gas that is substantially lower than the average CS density ρ . Momentum and mass conservation result in the maximal preshock velocity of the intercloud gas

$$u = \frac{1}{6} \phi v_s \frac{\rho}{\rho_{ic}}, \quad (6)$$

where v_s is the forward shock speed, ϕ is the ratio of the energy density of cosmic rays to the density of the shock kinetic energy $0.5\rho v_s^2$. For $v_s = 9000 \text{ km s}^{-1}$ and $\rho/\rho_{ic} = 5$ one needs $\phi \approx 0.2$ to produce the preshock velocity of $u \approx 1300 \text{ km s}^{-1}$ in the wind frame. This estimate demonstrates that velocities of absorbing gas up to 1900 km s^{-1} might be explained, if the line-absorbing gas is associated with the intercloud gas accelerated in the cosmic ray precursor.

6.3 Why intensities of Mg II and O I lines are similar?

Between days 22 and 60 intensities of Mg II 7889 Å and O I 7773 Å lines in SN 2006jc are comparable (cf. Anupama et al. 2008). Given similar ionization and excitation potentials of these species a straightforward implication of this fact is that the abundances of oxygen and magnesium are comparable. This indicates that we perhaps see the matter in which oxygen is strongly depleted by CNO burning. Indeed, massive stars at the boundary between helium core and hydrogen envelope have a zone, in which oxygen is depleted owing to CNO burning by a factor of 10–20 (cf. Hirschi et al. 2004; Meynet & Maeder 2003). The low abundance of hydrogen in the CSM around SN 2006jc is consistent with

the conjecture that we might see the matter with strongly depleted oxygen.

An alternative explanation is that Mg/O ratio is cosmic, and intensities of Mg II and O I lines are comparable because these lines are thermalized, i.e., level populations are close to Boltzmann distribution and lines are optically thick. The thermalization in a certain line occurs if $\epsilon_{21} N_s > 1$, where N_s is the average number of conservative scattering in the line before the photon escape, $\epsilon_{21} = q_{21} n_e / A_{21}$ is the thermalization parameter, and q_{21} is the collisional de-excitation rate. Using estimates based on the CSM density, pressure equilibrium, He I line intensity, and Boltzmann excitation of the lower level I estimate $\epsilon_{21} N_s \sim 10$ for the Mg II 7889 Å line on day 22. This confirms the possibility of the thermalization of Mg II and O I emission lines.

What explanation of the comparable intensities of Mg II and O I lines — similar abundances of oxygen and magnesium or thermalization — is correct remains an open question. The conjecture of the similar abundances of Mg and O seems to contradict to the fact that the narrow absorption is absent in Mg II 7889 Å, while it is present in O I 7773 Å (cf. Anupama et al. 2008).

6.4 Ejecta, presupernova and explosion

Our modelling of light curve and other properties of SN 2006jc does not permit us to constrain the ejecta mass and explosion energy, although models with the moderate energy $(1 - 2) \times 10^{51} \text{ erg}$ are preferred, if one admits that the dust forms in the CDS with the velocity of $\sim 10^4 \text{ km s}^{-1}$. Moreover, models of SN 2006jc with and without ^{56}Ni are plausible, although both have its own drawbacks. The model of a standard SN Ibc powered by ^{56}Ni decay faces problems if we identify the blue continuum with the emission of the CDS. Only the low mass ejecta $\leq 1 M_\odot$ could reconcile the radioactive model with the proposed scenario of the blue continuum. On the other hand the drawback of the model without ^{56}Ni is that it predicts unacceptably strong X-ray luminosity.

A more certain judgement on the source of SNe Ibn luminosity at the nebular epoch could be made in principle on the basis of the late time ($t > 200 \text{ d}$) photometry and spectra of SN Ibn. A deviation of the bolometric light curve from that predicted by the radioactive model would favour the CS interaction as a primary energy source. On the other hand uniformity of light curves and their correspondance to that expected for the radioactive model would favour the radioactivity. If the radioactivity as a primary energy source will be confirmed the second crucial question would remain, whether the ejecta is a standard SN Ibc or the object similar to our low mass model A3 with $\sim 1 M_\odot$ ejecta and ^{56}Ni mass of $\sim 0.3 M_\odot$. This issue could be elucidated by the late time spectra that may or may not reveal strong [O I] 6300, 6364 Å emission, the canonical feature of SN Ibc, at the nebular stage. The strength of this emission relative to Fe II line continuum would confirm or reject a picture of explosion of a standard SN Ibc slightly spoiled by CS interaction. The dust absorption could hamper this test, although it may well be that due to clumpiness of the dusty shell the attenuation will not be large at the late nebular epoch.

The CSM mass around SN 2006jc at the distance $r \leq 2 \times 10^{15} \text{ cm}$ in our models (Table 1) is in the range of

0.02 – 0.05 M_{\odot} . With the outflow velocity $v_w = 600 \text{ km s}^{-1}$ this mass had to be lost by pre-SN during the last year before the explosion with the rate of $\sim 0.02 - 0.05 M_{\odot} \text{ yr}^{-1}$ and kinetic luminosity of $\sim (2.5 - 6) \times 10^{39} \text{ erg s}^{-1}$. The outflow characteristics suggest extraordinary behavior of pre-SN. The pre-SN mass loss might be related with the bright outburst two years before the SN 2006jc explosion (Nakano et al. 2006; Foley et al. 2007; Pastorello et al. 2007). However, if the ejection episode was as brief as the optical outburst then the CS shell should be narrow and reside at the distance of about $4 \times 10^{15} \text{ cm}$ in contrast to our model which suggests a significant fraction of CSM in the close vicinity, at $r < 2 \times 10^{15} \text{ cm}$. Assuming the CS shell expansion velocity of 2400 km s^{-1} one gets the CS shell even farther out, at the distance of $\sim 1.6 \times 10^{16} \text{ cm}$ (Mattila et al. 2008).

A problem of a vigorous mass loss that precedes the SN explosion is familiar in relation with SNe IIn. Following the conjecture invoked for SN 1994W (Chugai et al. 2004b) one might suggest that in some cases, including SNe Ibn, the mass ejection by pre-SN is initiated by the flash of nuclear burning, e.g., of neon. However, the current theory of stellar evolution does not predict the violent mass loss of pre-SNe with initial masses $< 100 M_{\odot}$ (Heger et al. 2003). Only models of massive stars in the range of $100 - 140 M_{\odot}$ reveal the instability that could result in the strong nuclear outbursts and mass ejection (Heger et al. 2003). The physics is in pair production, which leads to infall, explosion of carbon and oxygen followed by mass ejection. These stars can experience several ejection episodes before the ultimate collapse and collisions between consecutively ejected shells could produce optical outburst resembling supernovae events (Heger et al. 2003). Recently, extremely luminous SN 2006gy was identified with a similar phenomenon (Woosley et al. 2007). It is not clear, whether such a scenario is applicable to SNe Ibn. If does, then these supernovae should be attributed to the CS interaction in the absence of ^{56}Ni . An important implication of this scenario is that the luminous massive helium star should remain at the position of SN Ibn.

An alternative scenario, in which SN explosion might be preceded by the vigorous mass loss, is a binary system in which a black hole experiences a merging with the helium core of a red supergiant. The supernova explosion in this case is presumably driven by the non-relativistic jets generated by the rapid disk accretion of the helium core material onto the black hole. In fact this possibility is a version of a merger scenario of gamma-ray bursts (Fryer & Woosley 1998; Fryer et al. 1999). The merging of a neutron star with a red supergiant leads to the similar scenario because the inspiraling neutron star that accrete at the Bondi-Hoyle accretion rate grows black hole already in the hydrogen envelope (Chevalier 1993; Fryer et al. 1999). The binary scenario predicts asphericity of ejecta caused by jets and of the CSM caused by the equatorial outflow from the common envelope.

7 CONCLUSIONS

The goal of this study was to present a model that might account for the unusual properties of SNeIbn including SN 2006jc. I argue that the CS interaction with a dense CSM is essential energy source for the early light curve of SN Ibn. I demonstrated that the CS interaction at the early

stage leads to the formation of the CDS which in turn is responsible for the smooth continuum of early SN 2006er and unusual blue bumpy continuum of SN 2006jc. I showed that the dust can form in the CDS at about day 50 in accord with observations. The modelling of the He I line profile affected by the dust absorption confirms a picture in which the line-emitting gas is associated with the CS clouds shocked and fragmented in the forward shock, while the dust is related with the fragmented CDS.

It should be stressed that scenario in which SN Ibn supernova is the explosion of a standard or luminous SN Ibc slightly modified by the CS interaction remains unconfirmed and photometry and spectroscopy of SNe Ibn at the late nebular stage are needed to clarify the issue.

ACKNOWLEDGMENTS

I am grateful to Ryan Foley for providing me spectra of SN 2006jc.

REFERENCES

- Anupama, G. C., Sahu, D. K., Gurugubelli, U. K., Prabhu, T. P., Tominaga, N., Tanaka, M. & Nomoto, K. 2008, arXiv e-prints, 811, arXiv: 0811.0060
- Arnett, W.D., 1980. ApJ, 237, 541
- Blondin, J. M., & Ellison, D.C. 2001, ApJ, 560, 244
- Chevalier, R. A., & Fransson, C. 1994, ApJ, 420, 268
- Chevalier, R. 1993, ApJ, 411, L33
- Chevalier, R. A. 1982a, ApJ, 258, 790
- Chevalier, R. A. 1982b, ApJ, 259, 302
- Chevalier, R. A., & Blondin, J. M. 1995, ApJ, 444, 312
- Chugai, N. N., Chevalier, R. A., & Utrobin, V. P. 2007, ApJ, 662, 1136
- Chugai, N. N., Chevalier, R. A., & Lundqvist, P. 2004a, MNRAS, 355, 627
- Chugai, N. N. et al. 2004b, MNRAS, 352, 1213
- Chugai, N.N. 2001, MNRAS, 326, 1448
- Cumming, R. J., Lundqvist, P., & Meikle, W. P. S. 1994, IAU Circ., No. 6057
- Di Carlo, E., et al. 2008, ApJ, 684, 471
- Draine, B. T. & Lee, H. M. 1984, ApJ, 285, 89
- Draine, B. T. & Salpeter, E. E. 1977, JChPh, 67, 2230
- Foley, R. J., Smith, N., Ganeshalingam, M., Li, W., Chornock, R. & Filippenko, A. V. 2007, ApJ, 657, L105
- Fryer, C. L., Woosley, S. E., & Hartmann, D. H. 1999, ApJ, 526, 152
- Galama T. J. et al. 1998, Nature, 395, 670
- Haines, J.R., Tsai, C.C. Graphite sublimation tests for muon collider/neutrino factory. 2002. Oak Ridge National Laboratory. ORNL/TM-2002/27
- Hasegawa H. & Kozasa T. 1988, PTPS, No. 96, 107
- Heger, A., Fryer, C. L., Woosley, S. E., Langer N., & Hartmann, D. H. 2003, ApJ, 591, 288
- Hirschi, R., Meynet, G., & Maeder, A. 2004, A&A, 425, 649
- Immmer, S. et al. 2008, ApJ, 674, L85
- Klein, R. I., McKee, C. F., & Colella, P. 1994, ApJ, 420, 213
- Mattila, S. et al. 2008, MNRAS, 389, 141
- Matheson, T., Filippenko, A. V., Chornock, R., Leonard, D. C., & Li W. 2000, AJ, 119, 2303
- MacFadyen, A. I., Woosley, S. E., & Heger, A. 2001, ApJ, 550, 410
- Meynet, G. & Maeder, A. 2003, A&A, 404, 975

- Nakano, S., Itagaki, K., Puckett, T., & Gorelli, R. 2006, Central Bureau Electronic Telegrams, 666, 1
- Nozawa, T. et al. 2008, ApJ, 684, 1343
- Pastorello A. et al. 2008, MNRAS, 389, 131
- Pastorello A. et al. 2007, Nature, 447, 829
- Pinto, P. A. & Eastman, R. G. 2000, ApJ, 530, 757
- Pozzo, M., Meikle, W. P. S., Fassia, A., Geballe, T., Lundqvist, P., Chugai, N. N. & Sollerman, J. 2004, MNRAS, 352, 457
- Smith, N., Foley, R. J., & Filippenko, A. V. 2008, ApJ, 680, 568
- Sutherland, R. S. & Dopita, M. A. 1993, ApJS, 88, 253
- Tabak, R. G., Hirth, J. P., Meyrick, G., & Roark, T. P. 1975, ApJ, 196, 457
- Tominaga N. et al. 2008, ApJ, 687, 1208
- Williams, R. E., Hamuy, M., Phillips, M. M., Heathcote, S. R., Wells, L., & Navarrete, M. 1991, ApJ, 376, 721